

Analysis of Heat and Moisture Transients in Paper During Copying and Digital Printing Processes

Sergiy A. Lavrykov and Bandaru V. Ramarao

Empire State Paper Research Institute, Department of Paper and Bioprocess Engineering, SUNY College of Environmental Science and Forestry, 1 Forestry Drive, Syracuse NY 13210
E-mail: bvrarama@esf.edu

Robert D. Solimeno

Immersitech LLC, 1775 Mentor Avenue, Cincinnati, OH 45212

Kapil M. Singh[^]

International Paper Co., 6283 Tri-Ridge Blvd., Loveland, OH 45140

Abstract. Modern digital copy machines are being designed to run at increasingly higher speeds. In this article, the authors analyzed the thermal and moisture content profiles and their evolution in paper sheets during the fusing process. The thermal parameters for the paper sheets necessary for the model were obtained by independent measurements. Model predictions for the evolution of sheet temperatures were compared with experimental measurements in a commercial large print run copier in order to establish the validity of the model. Sheet temperatures on the image and reverse sides were measured at different points in a continuous run Xerox photocopier. Sheet surface temperatures depend on basis weight, caliper, coating level and filler levels. Coated or highly filled sheets showed higher temperatures, which persisted for longer times, whereas those of lower densities were cooler. Moisture redistribution effects within the short time scale of fusing were insignificant. © 2013 Society for Imaging Science and Technology. [DOI: 10.2352/J.ImagingSci.Technol.2013.57.6.060546]

INTRODUCTION

Several processes subject paper sheets to thermal pulses. In paper drying, wet saturated paper sheets are subjected to a high temperature pulse on one surface. The newer high intensity drying processes rely on augmentation of the conventional drying mechanisms by pressure and capillary driven flows through the webs.¹ Paper sheets are subjected to similar thermal pulses in laser jet printing and photocopying applications. Here, toner particles on the sheet surface are fused to fasten the image by raising the surface temperature beyond the toner glass transition point. The surface temperature and thermal energy in the sheet determine the quality of the image and performance of the paper. The exposure of the sheet to a transient thermal pulse can cause it to curl, resulting in paper jams in copiers or printers. Transport models have been applied in the past to

calculate the evolving moisture and temperature profiles in these processes. The transport of heat and moisture through paper can be quite complex because of the porous and hygroscopic nature of paper fibers.² Models for heat and mass transport with application to drying of paper have been reported in the literature.^{3–7} However, only recently have comprehensive models for the thermal transients in fusing been developed.

Simula et al.⁸ reported an investigation of the temperature response of a sheet subjected to a hot roll nip. Their model was confined to transport in the thickness direction of paper and also considered only heat conduction through the composite medium. Furthermore, the validity of their simulation is restricted to short times since moisture diffusion and convective transport processes become significant at longer times. A more comprehensive simulation of the transient thermal, moisture and pressure fields inside paper sheets traveling through a hot roll nip was developed by Bandyopadhyay et al.⁹ Their simulation considered the complete transient two-dimensional temperature, moisture and air flow velocity fields within the paper sheets as they traveled through the fuser nip. The anisotropy in the transport properties of paper sheets for the in-plane and Z directions was also considered. The relevant energy, moisture and flow conservation equations were solved using a finite-volume method. The most important findings to emerge were that the temperature and moisture content fields were critically dependent on the sheet properties. However, the simulations were not verified by experimental measurements.

Recently, an investigation of heat and moisture transport in a paper sheet during exposure to a hot surface in printing was reported by Zapata.¹⁰ In this work, a model similar to the present one was proposed although the application was slightly different.

In order to understand the development of the temperature field during fusing in copying, we need simulations which are verified by suitable experimental data so that the

[^] IS&T Member.

Received Feb. 25, 2013; accepted for publication Nov. 12, 2013; published online Mar. 15, 2014. Associate Editor: George Chiu.

1062-3701/2014/57(6)/060504/8/\$25.00

Table of symbols

c_p	Specific heat of paper
c	Concentration of water vapor in pores
q	Concentration of moisture in fibers
D_p	Diffusivity of water vapor in pores, at temperature T
D_a	Diffusivity of water vapor in air, at temperature T
D_q	Diffusivity of moisture in fibers, at temperature T
D_{q_0}	Diffusivity constant
E_a	Activation energy for moisture diffusivity in fibers
k_i	Moisture transport coefficient
k_p	Thermal conductivity of paper
m	Index in diffusivity moisture correlation
$M_{GAB}, C_{GAB}, K_{GAB}$	Isotherm constants
q_s	Saturation value of moisture content of fibers, given by isotherm
R	Universal gas constant
T	Temperature
T_{ref}	Reference temperatures
ρ_p	Density of paper
α, β	Constants for temperature dependence of isotherm
k	Isotherm constant
λ	Enthalpy of adsorption at temperature T

effects of variation of the paper material and the fusing section variables can be systematically studied. In the present paper, we developed a simplified version of the earlier mathematical model and confirmed its predictions with experimental measurements of sheet temperatures in a high speed digital copier.

MATHEMATICAL MODEL FOR TRANSPORT IN THE FUSING SECTION

We consider a paper sheet which is initially at equilibrium at known moisture and temperature conditions, traveling through a nip consisting of hot and cold rollers as shown in Figure 1. The two rollers are kept at constant but different temperatures and expose the sheet to a temperature pulse on its surface as it moves through the nip. The paper sheet is a porous hygroscopic medium for analysis of the transport processes. The most important variables are the temperature $T(t, x, z)$ and the moisture content $q(t, x, z)$ fields. Since the pore space present in the paper sheet can hold water vapor, the concentration field $c(t, x, z)$ is also relevant. Although we track the evolution of these three fields, the experimentally measurable quantities are usually the temperatures at the top and bottom surfaces and the energy and moisture transferred to the environment. Our new model is enhanced compared to the earlier one of Bandyopadhyay et al.³ by considering the dynamics of the vapor space coupled with the moisture content of the fibers in the sheet through a separate diffusion mechanism.

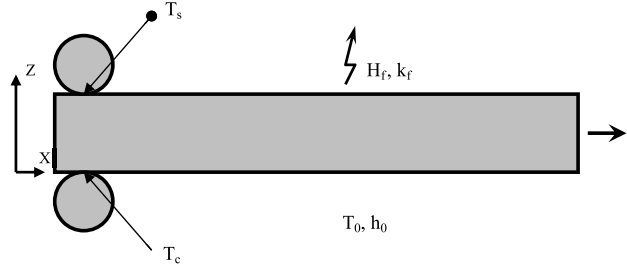


Figure 1. Schematic of the model domain, temperatures and external heat and mass transfer coefficients.

Model Equations

The equations for transient moisture transport are given below for the water in the pore space and fibers²:

$$\varepsilon \frac{\partial c}{\partial t} = D_p \nabla^2 c - \Gamma(q, T), \quad (1)$$

$$\frac{\partial q}{\partial t} = \nabla [D_q \nabla q] + \Gamma(q, T), \quad (2)$$

$$D_p = \frac{\varepsilon D_a(T)}{\tau}, \quad (3)$$

$$D_q = D_{q_0} e^{-\frac{E_a}{RT} + mq}. \quad (4)$$

In Eq. (1), the accumulation of water vapor in the pore space of the sheet is given by the first term. The second term represents the accumulation of moisture in the fibers and the third term represents the movement of water vapor by convection within the pore space. These are equated to the diffusion flux of water vapor in the pore space on the right hand side of the equation. The adsorption or desorption of moisture by the fibers is represented by Eq. (2). Here, moisture accumulation in the fibers is given by the left hand side. The first term on the right hand side represents moisture flux due to diffusion within the fiber space in all the dimensions and the second term $\Gamma(q, T)$ represents the local exchange of moisture between the fibers and the pores. This local exchange term can frequently be approximated by a linearized driving force approximation as used frequently in modeling the kinetics of adsorption in porous materials.¹⁰ This approximation can be written as

$$\Gamma(q, T) = k_i [q_s(c, T) - q]. \quad (5)$$

The above approximation states that the adsorption or desorption flux inside the material is proportional to the deviation of the local moisture content from the equilibrium value. The proportionality constant (denoted by k_i) has been determined as a fitting parameter in moisture sorption studies on similar paper materials.^{2,10} Convection of water vapor within the pore space is driven by local variations in the pore space pressure of the air–water vapor mixture, $P(t, x, z)$. When the temperature of the fibers changes locally, moisture is adsorbed or desorbed into the pore space in accordance with the equilibrium relationship.

The above equations allow for water vapor transport by diffusion and convection within the pore space and diffusion locally between the fibers and the pore space. When the

time scale for diffusion within the fibers is small, e.g., when the fiber phase is relatively thin, local equilibrium may be assumed.¹⁰ However, local equilibrium of moisture in non-isothermal situations is not likely to be valid although the fiber and pore spaces may be assumed to have the same temperature on account of the relatively high thermal conductivity of the fibers. The average thermal conductivity of the sheet is denoted by k_p and the heat capacity by c_p . The energy equation is given by

$$\rho_p c_p \frac{\partial T}{\partial t} = k_p \nabla^2 T + \rho_p \frac{\partial(\lambda q)}{\partial t}. \quad (6)$$

Since the moisture content of the fibers, especially in copy paper containing a significant amount of fillers, is small, we assume that the convection induced in the pore space is negligible, an assumption that will not be suitable for other situations such as drying and the changes occurring in significantly moist paper. The equilibrium relation between the moisture content and the water vapor content in the pore space and the local temperature is necessary. This relation, denoted by $q_s(c, T)$, is given by a modification of the Guggenheim–Anderson–de Boer isotherm employed earlier by Bandyopadhyay et al.⁹ The isotherm is given by

$$q_s = \frac{k(T)M_{GABC}}{(1 - K_{GABC})[1 + K_{GAB}(C_{GAB} - 1)c]}, \quad (7)$$

where

$$k(T) = \alpha e^{-\beta \frac{T_{ref,1} - T}{T_{ref,1} - T_{ref,0}}}. \quad (8)$$

The upper and lower temperatures are taken as 200°C and 21.8°C whereas the parameters α , β are fitted to experimental data on the isotherms. Although hysteresis is known to occur for moisture sorption in paper,^{11,12} for the purposes of these calculations it was neglected and the adsorption and desorption curves were assumed to coincide. Note that the magnitude of the hysteresis decreases with temperature and therefore this assumption should not impact the temperature and moisture profiles too severely.

Initial and Boundary Conditions

The paper sheet is assumed to be in equilibrium with its surrounding environment and is at a moisture content given by q_0 and temperature T_0 , both of which are uniform throughout. As the sheet travels through the nip region, the temperature of the top surface rises by contact with the hot roller, to T_h . In the post-nip region, the environment is at the initial conditions but heat and moisture can be transported by convection out of both of these boundaries. The relevant heat and mass transfer coefficients are assumed to be known. These were measured experimentally as discussed in the experimental section. The energy and moisture fluxes at the two boundaries are given by the following equations:

$$- [k_p \nabla T] \cdot \mathbf{n} = h_f (T_s - T_0), \quad (9)$$

$$- [D_p \nabla c + \rho_p D_q \nabla q] \cdot \mathbf{n} = k_f (c_s - c_0), \quad (10)$$

where the unit outward normal vector to the boundary is denoted by \mathbf{n} .

Table I. Baseline paper properties.

Parameter	Units	Value
Paper thickness	mm	0.1368
Ash content	%	8.69
Density	g/cm ³	0.773307
Porosity		0.5
Specific heat	J/(g K)	1.55
Thermal conductivity	W/(cm K)	0.001094
Thermal diffusivity	cm ² /s	0.000913
Enthalpy of adsorption	J/g	2.257 × 10 ³
D_p	cm ² /s	0.0053
D_{q0}	cm ² /s	5 × 10 ⁻⁸
m		232
K_i		0.003
M_{GAB}		0.05
K_{GAB}		0.8
C_{GAB}		80
RH_{init}	%	50
RH_{Amb}	%	50
k_f	cm/s	0.1
T_0	°C	20
h_f	W/(cm ² K)	0.001

The surface temperature and surface vapor concentration are denoted by T_s and c_s respectively. The surface vapor concentration is an additional variable in this equation which is defined as the value that is at equilibrium with the paper sheet at its local moisture content, $q_s(c_s, T_s)$ through Eq. (7).

Model Parameters

In order to investigate a baseline case, we used the model parameters given in Table I. The paper sheet thickness, porosity and other parameters were obtained from measurements of the thermal conductivity, heat capacity, moisture sorption equilibria and diffusivities of coated and uncoated copy papers.^{13,14} The other parameters were obtained from indirect or direct measurements of conditions inside typical copiers.⁹

MODELING RESULTS

The sheet response was characterized by the sheet surface temperature, the average sheet temperature, the average moisture content and how these parameters vary with sheet properties. These variables can be measured easily and thus serve to validate the model. The key sheet properties we varied were sheet thickness, sheet density, sheet thermal conductivity and heat capacity. Figure 2(a) shows the temperature of the hot roller applied to the sheet (denoted by T_h). This temperature rises rapidly, remains there as the nip travels over the surface and decreases back to the ambient value after the nip. Fig. 2(b) shows the temperature of the sheet's surface as a function of time as it travels through the nip region. The surface temperature increases rapidly

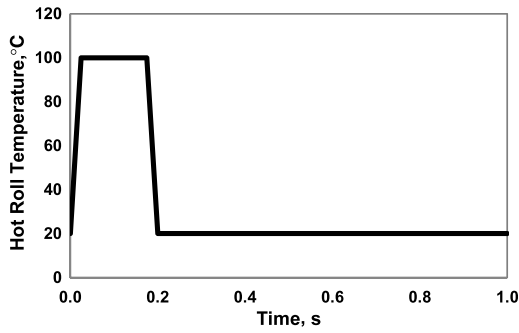


Figure 2a. Hot roller temperature at the surface during the nip.

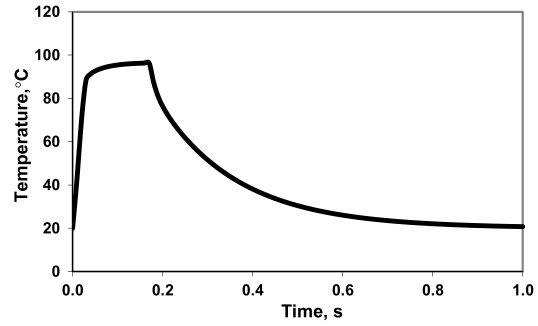


Figure 2b. Sheet surface temperature during and after it passing through the nip.

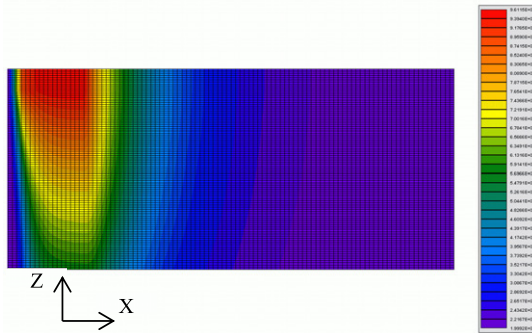


Figure 2c. Sheet temperature field during the hot roll nip.

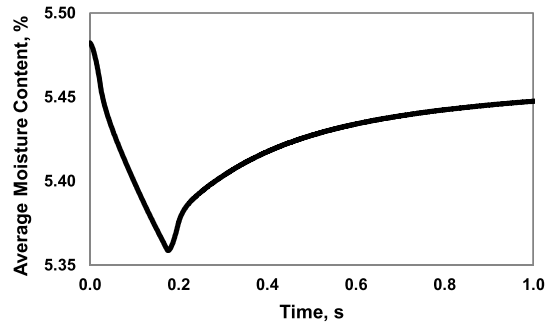


Figure 2d. Average moisture content of the sheet as a function of time.

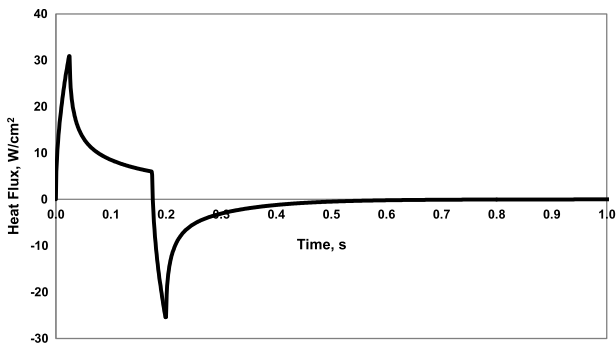


Figure 3. Heat flux on the top surface of the paper sheet.

to the roller temperature. The cool-down of the surface is much slower because it is governed primarily by the surface heat transfer coefficient in the post-nip region. This cooling curve determines the time that the surface remains hot for the fusion process. Fig. 2(c) shows the two-dimensional temperature field within the paper sheet at a time when the sheet has almost completed its travel. The pulse has reached a steady shape whereas the bulk of the sheet in the post-nip region has cooled rapidly. Fig. 2(d) shows the average moisture content within the sheet for these conditions. The moisture content decreases as the sheet heats up, but since moisture is mostly reabsorbed into the sheet as it cools down, the net loss in moisture content is relatively small. Figure 3 shows the heat flux to the top surface of the sheet during the travel. The flux rises rapidly within a short time interval corresponding to the rise time of the contact temperature. This increase is because the sheet's surface temperature is

much lower than the hot roller temperature during this time. The flux decreases after the surface reaches the hot roller's temperature because the gradient in temperature at the surface has moderated during this time interval. The surface contact temperature drops when the sheet leaves the nip resulting in a steep decrease in the heat flux. The flux becomes negative, i.e., the sheet begins to lose heat to the surroundings in the post-nip region. The heat loss to the environment moderates as the surface cools to the ambient temperature, showing a slower exponentially decreasing negative heat flux in the after nip region. Figure 4(a) shows the time variation of surface temperature for sheets of different specific heats. Higher heat capacities and densities tend to damp the rise in temperature and slow the dynamics. Both heat-up and cool-down are affected and thus slowed. Increased sheet thickness has an interesting effect on the surface temperature. Fig. 4(b) shows the impact of changing the sheet thickness on the surface temperature. Fig. 4(c) and (d) show the corresponding temperature fields in two dimensions for a thin and a thick sheet. For very thin sheets (20 μm), the temperature pulse penetrates completely and the sheet reaches a uniform temperature. As sheet thickness increases, the depth of penetration decreases, and for very thick sheets (>200 μm), the sheet may be considered as a semi-infinite body.

EXPERIMENTAL PROCEDURE

In order to provide a more precise and carefully controlled experimental verification of the model, a commercial copier (Xerox Docutech 6180) was instrumented with four

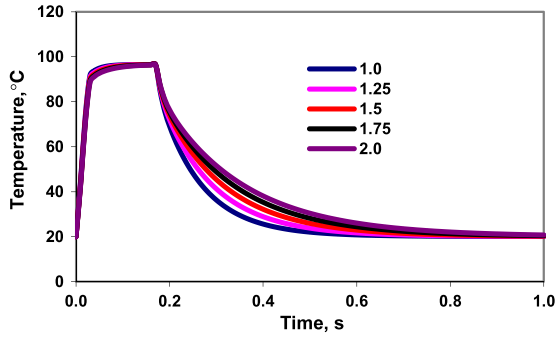


Figure 4a. Sheet surface temperature for different sheet specific heats (J/gK).

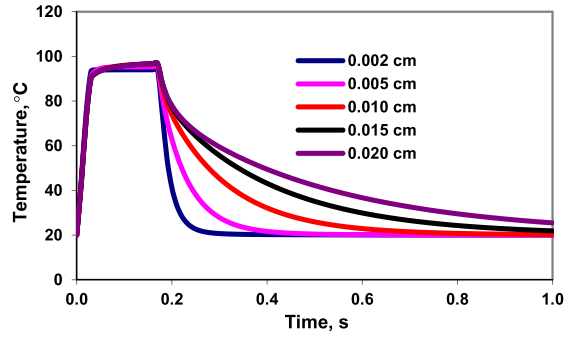
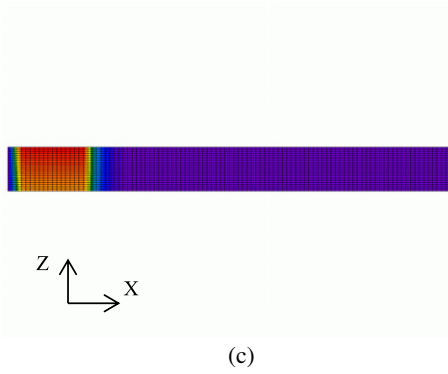
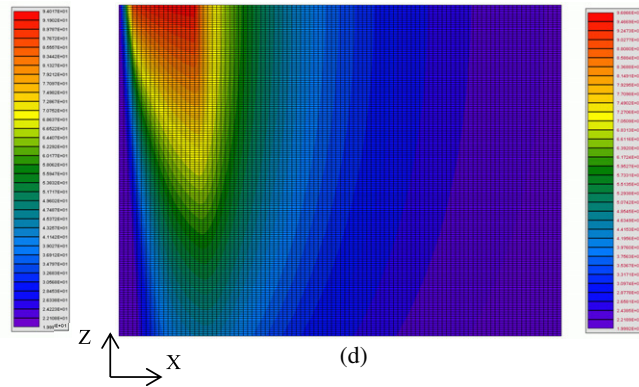


Figure 4b. Sheet surface temperature for different sheet thicknesses (cm).



(c)



(d)

Figure 4c & d. Temperature fields in sheets with 0.002 (c) and 0.015 cm (d) thicknesses.

Table II. Paper types, their properties, experimental measurements and model predictions of sheet surface temperatures in the continuous run copier.

Paper ID	Description	Basis weight (g/m ²)	Caliper (μm)	Density (kg/m ³)	Filler content (%)	Conductivity (W/(m K))	Specific heat (kJ/(kg K))	Press roll temp (°C)	Average temp (°C)	
									Expt	Model
Paper 1	Uncoated 1 (Vector 20)	75.6	98.8	765.1	20.7	0.11	1.4	72.7	91.3	91.06
Paper 2	Coated Cover (CC Cover 60)	165	173.2	951.9	27.8	0.175	1.1	53.3	70.2	69.61
Paper 3	Coated Cover (CC Cover 80)	222	220.2	1005.8	26.9	0.22	1	51.4	65.3	63.35
Paper 4	Glossy Cover (Digital gloss cover)	212	198.6	1067.8	21.6	0.245	1	46.5	66.9	65.07
Paper 5	Uncoated 2	75.7	94.3	803.4	22.3	0.0968	1.2	77.6	88	88.68
Paper 6	Uncoated 3	88.6	113.3	784.4	23.1	0.0972	1.2	77.1	76.4	78.48

temperature sensors connected to two computers through data acquisition systems. Two sensors were inserted in the cabinet at different locations near the paper path and close to the fuser roll. An infrared sensor connected to a T type thermocouple was used to sense the temperature at the surface of the paper sheet as it came out of the fuser section. A Fluke 576 Precision Infrared thermometer was mounted separately and targeted at the surface of the pressure backing roll using a laser ranging sensor. This was connected to a separate computer and data for the surface temperature of the backing roll were acquired. Figure 5(a) shows a picture of the internals of the copier with the sensors attached. Fig. 2(b) is a schematic showing the locations of the sensors. Table II shows the characteristics of the paper sheets used for this

test. These were commercially available copy paper and were identified as samples 1 through 4.

EXPERIMENTAL RESULTS AND COMPARISON WITH MODEL PREDICTIONS

Figure 6(a) shows the four temperatures measured by the sensors for paper sample 1. The copier was run for 1000 copies. The paper was a standard copy paper (paper 1) whose properties are listed in Table II. It took approximately 500 copies for the temperature of the sheet surface to reach a steady state. The ambient temperatures were constant at 25°C. The paper surface was at 90°C and the pressure roll was at 65°C. The pressure roll surface temperature decreased with time until it reached a steady state. During the heat-up



Figure 5a. Picture of the interior of a Xerox Docutech 6180 with sensors placed in the paper path.

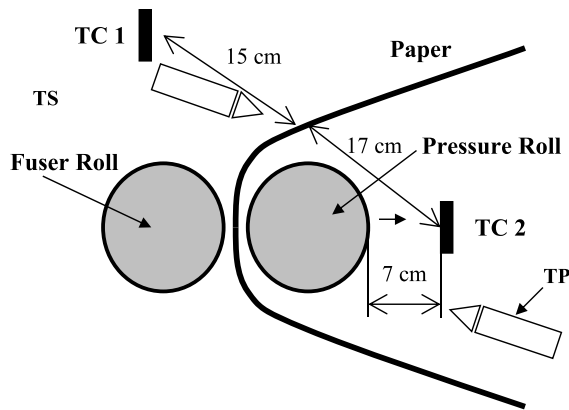


Figure 5b. Sketch of the various sensors. TC1—thermocouple (T type) for measuring ambient environmental temperature near the paper surface. TC2—thermocouple (T type) for measuring ambient temperature near the pressure roll. TS—IR sensor with K type connector for the paper surface after the fuser (approx. 8 cm). TP—IR camera sensor with laser ranging (temperature of pressure roll).

period when no copying occurs, the pressure roll and the fuser roll are in (imperfect) thermal contact, which results in heating of the pressure roll to an initially high temperature. The pressure roll temperature decreases with time as it loses heat to the paper sheets. Fig. 6(b) shows the paper surface temperature for the paper samples 1 through 4. The surface temperature was highest for sample 1, which had the smallest caliper, basis weight and density. These sheets tend to have the least thermal capacity and can heat up more rapidly than heavier grades. Samples 2 and 3 are cover copy paper with higher basis weights. The surface temperatures are significantly lower in these cases. Sample 4 is a glossy copy paper with high filler level, which causes higher thermal conductivity and sheet density, although the specific heat tends to be lower.⁵ The sheet surface temperature is higher than its counterpart cover stock (80 lb). The pressure roll temperature decreases with each of these sheets, as shown in Fig. 6(c). The decreased temperature is due to the higher sheet thermal capacities as well as higher sheet thicknesses. Both of these serve to lower the bottom surface temperature

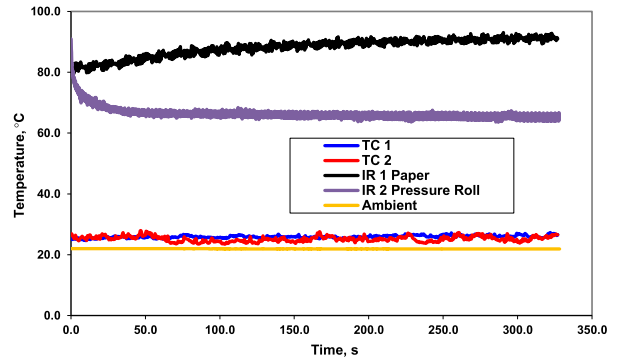


Figure 6a. Temperatures of various sensors with the machine running paper 1. The paper surface (IR 1) is at the highest temperature. The copier achieves a steady state after about 700 copies. It is run for 1000 copies. Ambient, TC1 and TC2 are approximately the same. The copier speed is 180 ppm.

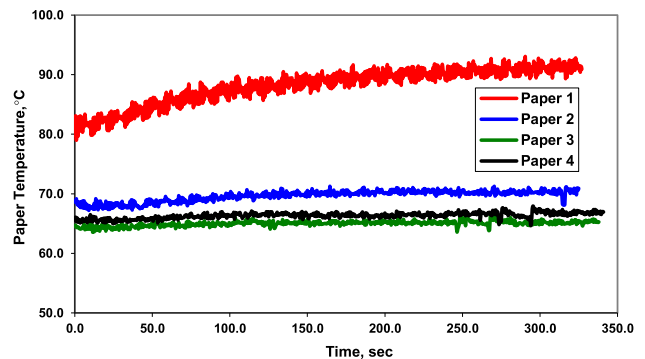


Figure 6b. Temperature of the paper surface for different copy paper grades. Heavier paper grades (higher BW) result in smaller surface temperatures. The paper 4 sheet has higher surface temperature probably due to higher thermal conductivity (higher thermal diffusivity also).

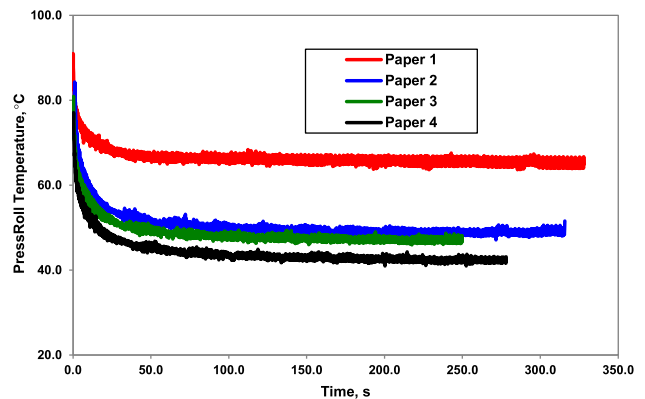


Figure 6c. Press roll temperature for different paper sheets. The press roll temperature also decreases with increased BW. However, paper 4 shows the smallest temperature whereas paper 3 is higher. This may be because the thermal pulse in the coated paper gets dissipated in the top layer and does not penetrate deep enough into the base sheet. The magnitude of oscillations for paper 1 is highest. The magnitude of oscillations decreases with BW.

of the paper sheets as they travel through the fuser section. Figure 7 summarizes all the experimental measurements for the temperatures for the paper sheets. The fluctuations are

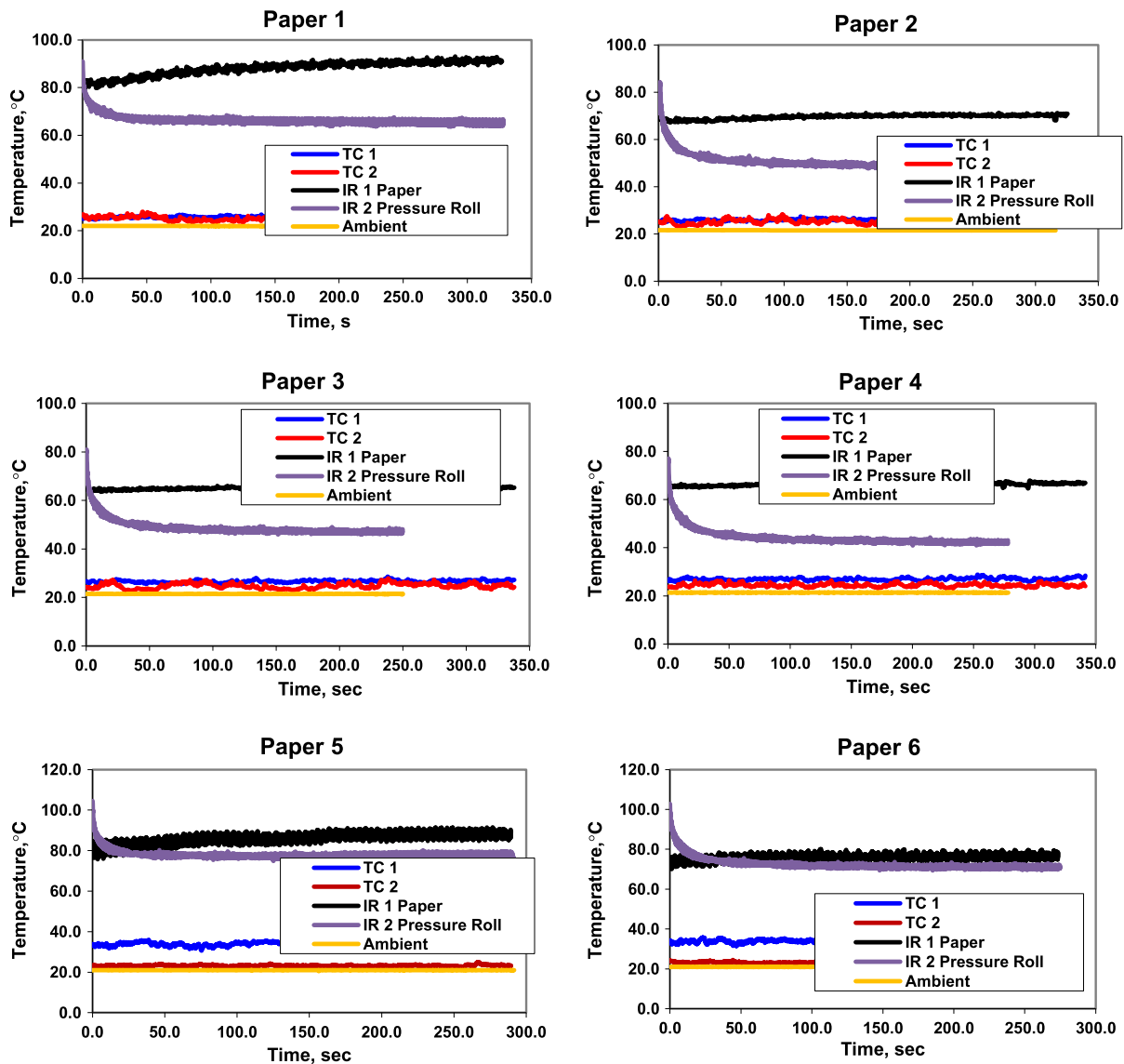


Figure 7. Temperatures within the copier for each paper grade.

caused by the gaps between the sheets during their travel as well as the modulation of the temperature measurements by the response characteristics of the thermometers (IR and thermocouples). By comparison, we observe that the magnitude of the fluctuations decreases with increased thermal mass and conductivity of the sheets. This is expected from the transient thermal response of paper sheets.

Table II shows also the average sheet temperature on the top surface of the paper as measured by the sensor and also the corresponding average calculated by the mathematical model. A very close correspondence between the surface temperatures was obtained.

CONCLUSIONS

The thermal response of the sheets can be seen to be strongly impacted by the sheet properties. In particular, the sheet basis weight, density, thermal conductivity and heat capacity are critical in determining this response. Since the thermal

properties are dependent on the sheet moisture content, the response would also be sensitive to the moisture content, although this was not directly investigated in this work.

REFERENCES

- 1 S. Ramaswamy and J. D. Lindsay, "The role of vapor formation in high-intensity drying — description and comparison of two models," *Nordic Pulp Paper Res. J.* **13**, 299 (1998).
- 2 B. V. Ramarao, A. Massoquete, S. Lavrykov, and S. Ramaswamy, "Moisture diffusion inside paper materials in the hygroscopic range and characteristics of diffusivity parameters," *Dry. Technol.* **21**, 2007 (2003).
- 3 S. Ramaswamy and R. A. Holm, "Analysis of heat and mass transfer during drying of paper/board," *Dry. Technol.* **17**, 49 (1999).
- 4 S. Ramaswamy and R. A. Holm, "High intensity drying," *Dry. Technol.* **17**, 73 (1999).
- 5 S. A. Reardon, M. R. Davis, and P. E. Doe, "Construction of an analytical model of paper drying," *Dry. Technol.* **17**, 655 (1999).
- 6 M. Harrmann and S. Schulz, "Convective drying of paper calculated with a new model of the paper structure," *Dry. Technol.* **8**, 667 (1990).

- ⁷ B. Wilhelmsson and S. Stenström, "Heat and mass transfer coefficients in computer simulation of paper drying," *Dry. Technol.* **13**, 959 (1995).
- ⁸ S. Simula, J. Ketoja, and K. Niskanen, "Heat transfer to paper in a hot nip," *Nordic Pulp Paper Res. J.* **14**, 273 (1999).
- ⁹ A. Bandyopadhyay, B. V. Ramarao, and E. Shih, "Transient temperature, moisture and pressure fields in a paper sheet exposed to a traveling thermal pulse," *J. Imaging Sci. Technol.* **45**, 598–608 (2001).
- ¹⁰ S. Lavrykov and B. V. Ramarao, "Axi-symmetric pore-fiber model for transport processes in paper," *Nordic Pulp Paper Res. J.* **19**, 506 (2004).
- ¹¹ S. G. Chatterjee and B. V. Ramarao, "Hysteresis in water vapor sorption equilibria of bleached kraft paper board," *Proc. 3rd Int'l. Symp. on Moisture and Creep Effects on Paper, Board and Containers* (APPITA, Rotorua, New Zealand, 1997), pp. 121–130.
- ¹² S. G. Chatterjee, B. V. Ramarao, and C. Tien, "Water vapor sorption equilibria of a bleached kraft paper board — a study of the hysteresis region," *J. Pulp Pap. Sci.* **23**, J 366 (1997).
- ¹³ S. Lavrykov and B. V. Ramarao, "Parameters for heat and moisture transport in paper sheets subjected to a temperature pulse in a hot-roll nip," *Proc. Int'l. Paper Physics Conf. & 61st APPITA Conf.* (Gold Coast, Australia, 2007), pp. 155–160.
- ¹⁴ S. A. Lavrykov and B. V. Ramarao, "Thermal properties of copy paper sheets," *Dry. Technol.* **30**, 297 (2012).